Penerbit Akademia Baru

Journal of Advanced Research in Fluid Mechanics and Thermal Sciences

Journal homepage: www.akademiabaru.com/arfmts.html
ISSN: 2289-7879

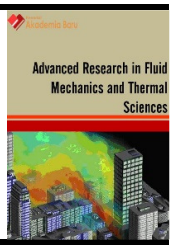

Haemodynamics Behaviour in Normal and Stenosed Renal Artery using Computational Fluid Dynamics

Open Access

Shah Mohammed Abdul Khader[1,*], Adi Azriff[1], Cherian Johny[2], Raghuvir Pai[2], Mohammad Zuber[3], Kamarul Arifin Ahmad[4], Zanuldin Ahmad[1]

[1] Department of Mechanical Engineering, School of Science and Engineering, Manipal International University, Malaysia, 71800, Nilai, Negeri Sembilan, Malaysia
[2] Department of Mechanical and Manfacturing Engineering, Manipal Institute of Technology, Manipal Academy of Higher Education, Manipal, 576104, Karnataka, India
[3] Department of Aeronautical and Automobile Engineering, Manipal Institute of Technology, Manipal Academy of Higher Education, Manipal, 576104, Karnataka, India
[4] Aerospace Engineering Department, Faculty of Engineering, Universiti Putra Malaysia, 43499 Selangor, Malaysia

ARTICLE INFO

Article history:
Received 29 June 2018
Received in revised form 15 August 2018
Accepted 17 August 2018
Available online 6 November 2018

Keywords:
Haemodynamics, renal artery, exercise and resting condition, Atherosclerosis

ABSTRACT

Atherosclerosis is a condition of plaque/fatty deposit on the walls of the artery resulting in obstruction to blood flow. Several researchers have studied the hemodynamic behaviour on patient-specific models. The aim of present study is to investigate the hemodynamic behaviour in 3D models of an idealistic abdominal aorta with renal branches based on (Computed Tomography) CT image. A new technique is used to develop the idealistic model from the single slice. Further, two more 3D models are generated by including stenosis in one renal branch and both renal branches separately. The investigation is focused on haemodynamics parameters such as flow field, pressure and Wall Shear Stress (WSS). The flow variables are monitored throughout pulsatile flow subjected to both resting and exercise cases. The obtained results from this fundamental study agree well with the available literature and can be useful for further studies.

1. Introduction

Atherosclerosis is found to be major cause of death rate globally. It is the condition in which plaque formation generally occurs close to bifurcations and curvatures [1]. In such diseases, the affected arteries get hardened as a result of accumulation of fatty substances inside the lumen or because of formation of plaques [2]. The growing interest to understand the biomechanics of generation, detection and the treatment of stenosis vascular diseases combined with advanced computational simulations has helped the medical doctors/biomedical engineers in developing the bio-medical instruments for treatment (surgical) modalities [3]. Existing clinical imaging modalities

* *Corresponding author.*
E-mail address: smak.quadri@gmail.com (Shah Mohammed Abdul Khader)

such as CT/MRI and Ultrasound Imaging techniques in coupling with the numerical simulation such as CFD can enhance the understanding of detailed physiology of blood flow in diseased vessels [4]. Many of the previous studies have demonstrated the feasibility of computational methods such as Computational Fluid Dynamics (CFD) technology in the haemodynamics simulation based on image data obtained from MRI/CT data [5]. Haemodynamics study using CFD shall provide the valuable information to doctors to understand the mechanisms of stenosis development and progression in patients.

In normal abdominal artery branching into renal arteries, the haemodynamic variables like mass flow rate, pressure difference and velocity were under normal physiological range. However, stenosis observed in renal artery is very important issue as it is linked with secondary hypertension. In addition, renal stenosis has also demonstrated the pressure & velocity increase and mass flow rate decrease with the higher percentage of stenosis [6]. The angulation effects of stenosed renal artery based on the velocity of blood and renal mass flow was also investigated [7]. It is found that, with larger renal angle, the arteries fail to deliver insufficient amount of blood to the kidney resulting in lower blood flow to kidney and causing activation of renin-angiotensin system leading to hypertension. Another study supported similar observation [8,9], which investigated the effect of renal artery stenosis on the vessel wall and flow dynamics. Pulsatile flow boundary condition was applied on patient-specific model which was reconstructed from CT images and used to investigate the fluid-structure interaction.

Comparative haemodynamic study in severe stenosed renal artery is also investigated [10]. The flow behavior was studied before renal artery stenosis, with presence of renal artery stenosis and after stent implantation. The presence of stenosis increased the flow resistance, pressure gradient and leads to low blood flow rates. After implantation, flow resistance decreases at level proportional to healthy artery. The influence of renal artery ostium flow diverter upon investigation to observe hemodynamics characteristics Lee and Chen [11] demonstrated that diverter shall direct the flow to the renal branches and also influence the flow pattern and recirculation, which are prime criteria causing to atherogenesis.

Haemodynamics has also been studied during rest and exercise conditions especially in abdominal aorta model for different flow conditions [12]. Flow recirculation zone and low wall shear stress was observed along the posterior wall of the infrarenal abdominal aorta in resting conditions and disappeared during exercise flow conditions. Further, this study was also extended to idealize abdominal aorta model in resting, light exercise, and moderate exercise pulsatile flow conditions. In these studies, the changes in the flow velocity field, the spatial variations of wall shear stress, and the temporal oscillations of wall shear stress were described in detail, and the effect of exercise was also determined. In another study for idealistic abdominal aorta with peripheral branches, was investigated and compared the regions having low WSS and flow recirculation with previous studies [13]. Supporting this study, it was hypothesized that, exercise shall helped in retardation of cardiovascular disease progression by reducing WSS and flow recirculation [14]. Flow reversal region was observed close to renal arteries and along the posterior wall under resting condition. However, during exercise condition, flow reversal was observed in proximal to abdominal bifurcation. Also, the lowest wall shear stress was observed close to renal arteries and lateral wall of the iliac artery and was highest at the branches. WSS of pulsatile flow was investigated using MR velocity for patient specific abdominal aorta model to study the haemodynamics in infrarenal segment of arteries [15].

The WSS was oscillated in the direction throughout the infrarenal aorta and prominent in the distal region. Exercise condition causes the changes the magnitude and pattern of WSS in distal abdominal aorta. Low limb exercise was recommended based on simulation study in an idealistic abdominal aorta with peripheral branches using CFD at rest and exercise condition. As observed in

previous studies, recirculation zone was found along the posterior wall of abdominal aorta immediately distal to the renal vessel under resting conditions [16]. Low time-averaged WSS was also observed in this location, posterior wall opposite to inferior mesenteric artery and along the anterior wall between the superior and inferior mesenteric arteries [17]. Low WSS and high OSI along the posterior wall distal to the renal arteries remained and under moderately exercise condition this got eliminated. Based on this observation, moderate lower limb exercises was beneficial to eliminate the low WSS and flow recirculation, which existed during resting condition [18].

However, rest and exercise condition is hardly investigated with focus on normal and different renal artery stenosis alone as observed in previous studies. Hence, the present study attempts to carryout fundamental investigation to understand the haemodynamics in idealistic abdominal aorta with renal artery branching for normal and different stenosed cases under resting and exercise condition. The comparison of results obtained for various stenosed severities reveals the high WSS zones on the far wall of downstream of the throat causing degradation of wall tissue. Also shear layer dissipates more quickly due to formation of high eddies in downstream. The flow behavior changes abruptly with the increase in velocity at throat and large recirculation in the downstream of stenosis. Moreover it is also observed that severity less than 75% is considered as mild and anything greater than this is termed as critical. This type of study will be useful to predict the outcome of severity of stenosis, and aids the physicians with better insight into flow dynamics. Numerical simulations thus aid in evaluating the hemodynamic variables for different stenosis conditions and the results were compared with normal renal artery.

2. Methodology

In the present study, blood flow is assumed to be incompressible, Newtonian fluid [19]. The dynamic flow is governed by the continuity and Navier-stokes equations [1, 20], respectively as

$$\nabla . u = 0 \tag{1}$$

$$\rho \left(\frac{\partial u}{\partial t} + u . \nabla u \right) = -\nabla p + \mu \nabla^2 u \tag{2}$$

Where ρ is the density, p is the pressure, μ is the viscosity and u is the velocity.

3D geometry of idealistic abdominal aorta with the renal branch is constructed from a single mid-slice of CT image and the configuration of the model is shown in Figure 1(a). The detailed dimensions of the idealistic model with mid-surface details is described in Figure 1(b). Due to the complexity of the model, the entire model has split it into 3 zones, such as zone A is the abdominal aorta, zone B is the right renal branch and zone C is the left renal branch. The splitting of the geometry is done using ANSYS Design Modeler [21]. Figure 2(a) shows the 3D model of normal idealistic abdominal model with renal branches after geometry cleanup and surface refining.

In Figure 2, region -1 and 2 highlights the abdominal artery, region-3: left renal artery and region -4: right renal artery. Single stenosed model describes the virtually generated in right renal artery with 71 % stenosis as show in encircled zone, region-4 of Figure 2(b). Details of stenosis: stenosis diameter of 0.315 times the renal diameter and length of 1.125 times the renal diameter as shown in the Figure 2(b). Double stenosed model describes the virtually generated stenosis in right artery having same % of stenosis as that of single stenosed case as shown in the encircled zone, region-4 of Figure 2(c). However, left renal artery consists of 78% of stenosis having stenosis diameter of 0.3

times the renal diameter and stenosis length of 1.65 times the renal diameter as shown in the encircled zone, region-3 of Figure 2(c).

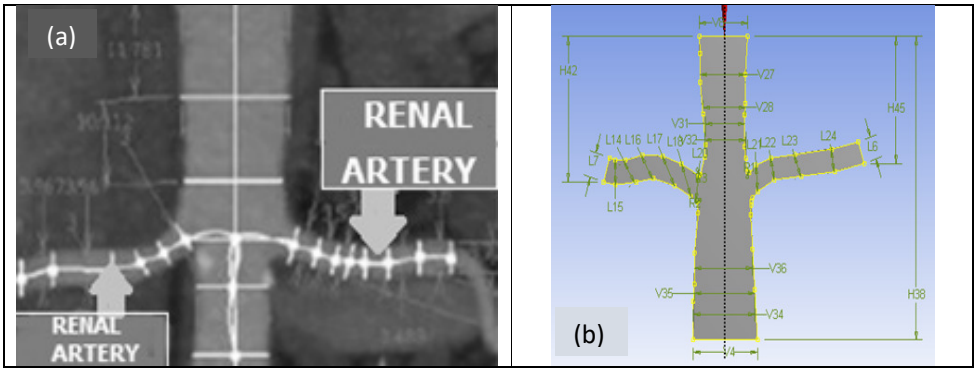

Fig. 1. CT data details (a) Geometry from CT Slice (b) Dimension lines illustrated for single slice of CT Scan Image in ANSYS Design Modeler

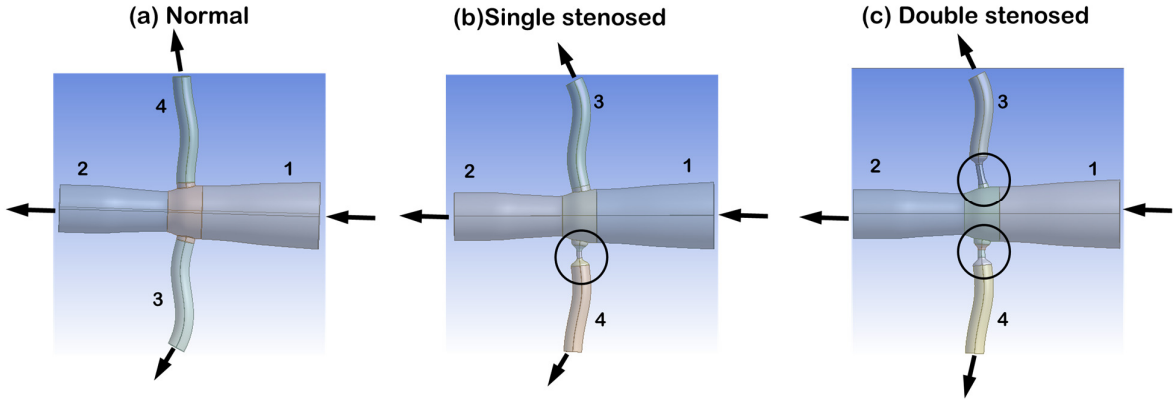

Fig. 2. Geometric description of various CFD models

Flow variables such as velocity and pressure are monitored for different grid sizes under steady state condition for normal and both the single and double stenosed conditions using ANSYS FLUENT. Reynolds number of 400 is applied at inlet and constant pressure of 90mmHg is applied at outlet. All the models are discretized into structured and unstructured mesh. Figure 3 shows the structured and unstructured mesh of normal abdominal aorta with renal branches. Details of mesh closer to wall to capture the effects of flow behavior is shown in the highlighted portion. Convergence criterion of 10^{-5} is used in the present study. Normal, single and double stenosed models are meshed with 355000, 385000 and 394500 structured and unstructured elements respectively.

In the present study, blood flow is assumed to be Newtonian even though it is non-Newtonian physiologically as the focus in on large arteries and hence, Newtonian assumption is acceptable as relatively high shear rate occurs. In medium and smaller arteries, non-Newtonian assumption is valid as shear rate is lower than $100s^{-1}$ and shear stresses depend non-linearly on the deformation rate. The density and dynamic viscosity of the blood is considered to be 1050 kg/m^3 and 0.004 N-sec/m^2 respectively [1,22].

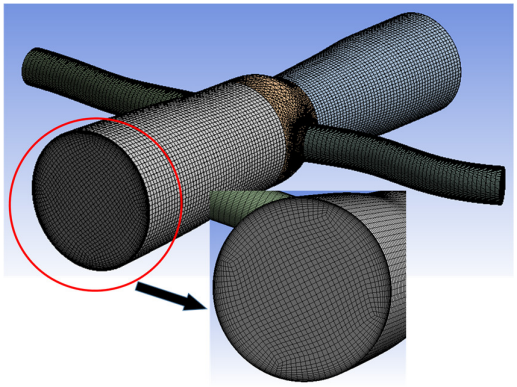

Fig. 3. Grid details of abdominal aorta with renal branches

Pulsatile time varying velocity profile as shown in the Figure 4 is applied at the inlet. Two different inlet pulsatile velocities are carried out separately under rest and exercise conditions. The transient analysis under rest condition is performed with pulse cycle of 0.9 sec. In exercise condition, pulse cycle will is 0.5 sec and the flow is observed with two-fold increase. Also, to include the peripheral resistance, a time varying pressure wave form is applied at the outlet as shown in the Figure 5 [3]. Each pulse cycle during rest and exercise conditions is discretized into 180 time steps to simulate the flow behavior more accurately. A user-defined function is developed to provide the pulsatile inlet velocity profile for rest and exercise condition and also pulsatile outlet pressure. These simulation results provide useful data in quantifying the haemodynamic changes in understanding the haemodynamics in abdominal aorta renal bifurcation.

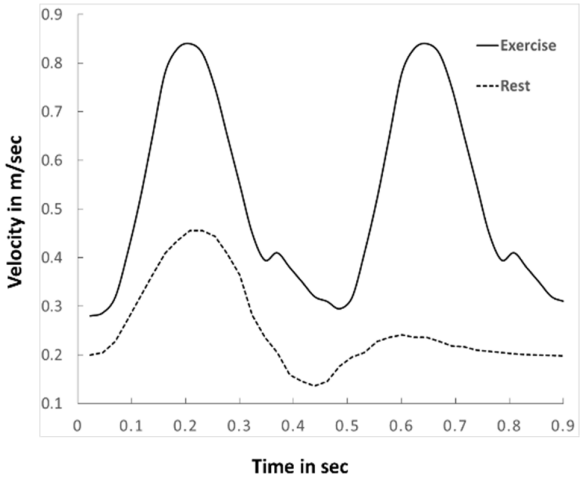

Fig. 4. Time varying inlet velocity

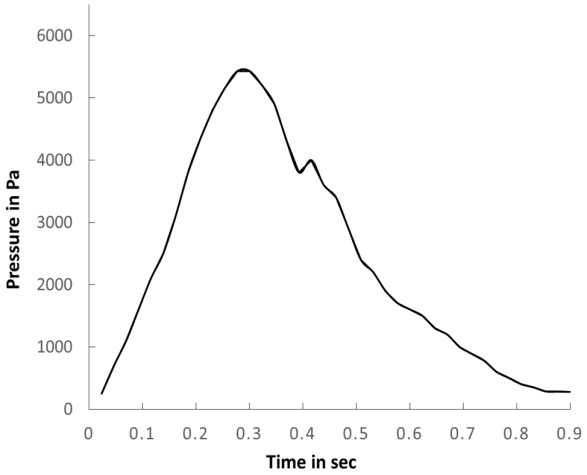

Fig. 5. Time varying outlet pressure

3. Results

Numerical simulation of different models with rest and exercise conditions is carried out for three pulse cycle and results obtained in the last cycle is considered for the investigation. The haemodynamics parameters like velocity, wall shear stress and pressure are studied at specific instants of pulse cycle like early systole, peak systole, early diastole and late diastole. These parameters varies with time due to the pulsatility of the flow waveform and the maximum value generally occurs at the peak systole when the inflow is maximum.

Figure 6 and 7 compares the flow velocity profiles at peak systole during rest and exercise conditions respectively in normal, single and double stenosed abdominal aorta models with renal bifurcation. Flow during pulse cycle in normal model is characterized by flow separation as flow divides into two streams entering into both the renal branches. Also maximum velocity is found to be at the distal wall side of renal bifurcation and slower moving fluid on the proximal wall side [11,23]. Flow in stenosed renal branch of the single stenosed model, is characterized by increased velocity at the stenosed site and flow recirculation in the downstream side. However, flow in renal branch on the normal side is similar to the flow observed in both normal renal branches. In rest conditions, flow jet at stenosed throat extends relatively to longer distance in double stenosed branches when compared to that in single stenosed branch [10,22,24]. In exercise condition, there is significant change in the flow jet extending to longer length in contrast to that in rest condition. Flow recirculation in downstream side of renal branches has also significantly reduced in exercise condition when compared with the rest condition. Flow velocity profile in downstream side of abdominal aorta has altered in double and single stenosed case when compared with the normal case which is found to be more intense in exercise condition in contrast to rest condition. In cardiac pulse cycle, flow separation is found to be more visible during peak systole and deceleration, however later it drops at the diastole phase. These changes in blood flow patterns have been linked to the growth of atherosclerosis.

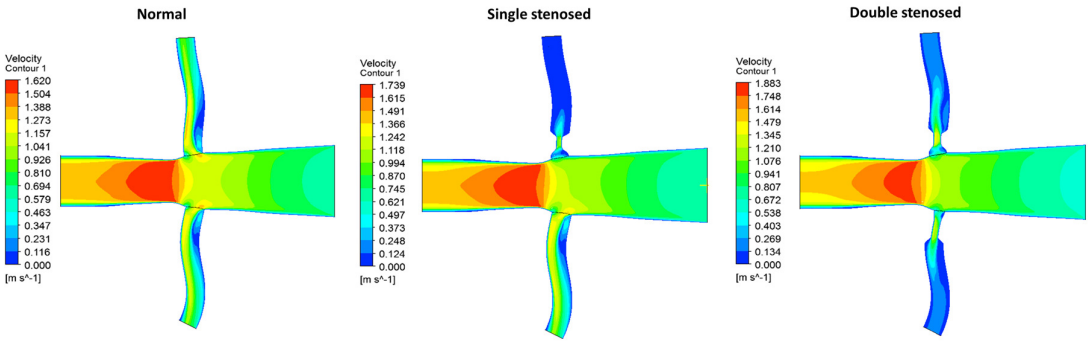

Fig. 6. Comparison of velocity contour during peak systole in rest condition in different models

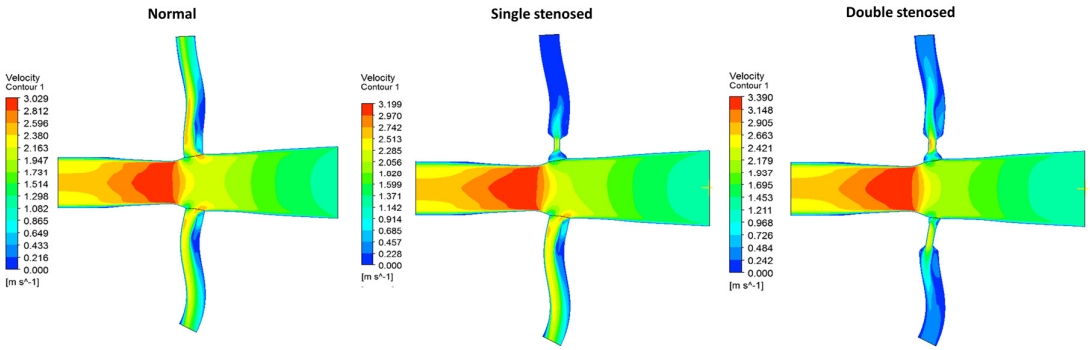

Fig. 7. Comparison of velocity contour during peak systole in exercise condition in different models

Figure 8 and 9 compares the maximum flow velocity in rest and exercise conditions at different locations such as 1, 2, 3 and 4 in complete cardiac cycle for normal, single and double stenosed models. It is observed that, flow velocity at location 1 and 2 reveals the flow pattern similar to the input velocity pulse cycle both in rest and exercise conditions. However, in renal branch location *i.e.* 3 and 4, in downstream side, significant difference in flow behaviour can be revealed between stenosed and normal models. In both fig.9 and 10, flow velocity at location 3 and 4 is higher in normal

model and drops slightly and considerably in single and double stenosed models. Flow velocity pattern also varies significantly in single and double stenosed when compared with the normal model pattern.

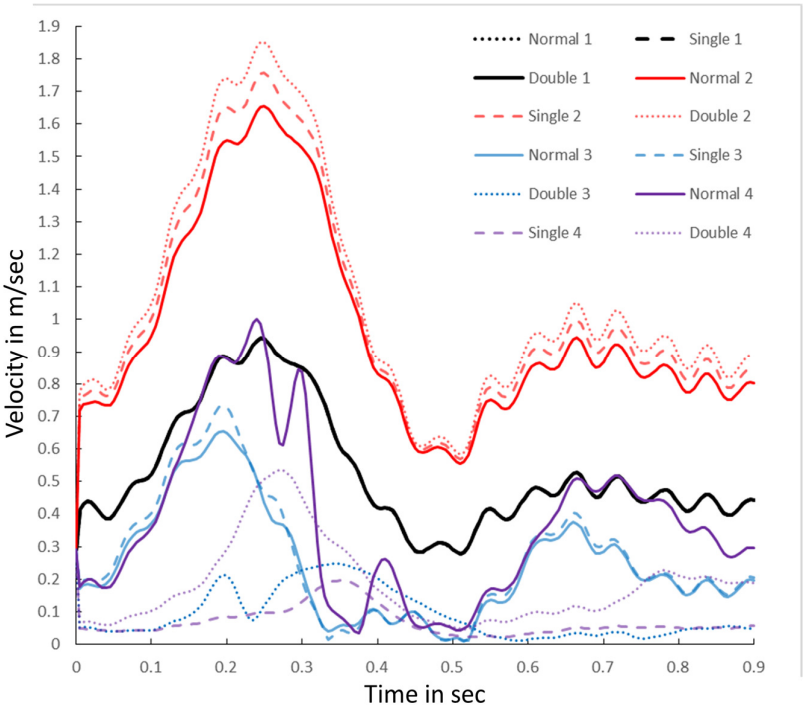

Fig. 8. Comparison of flow in pulse cycle during rest condition in different models

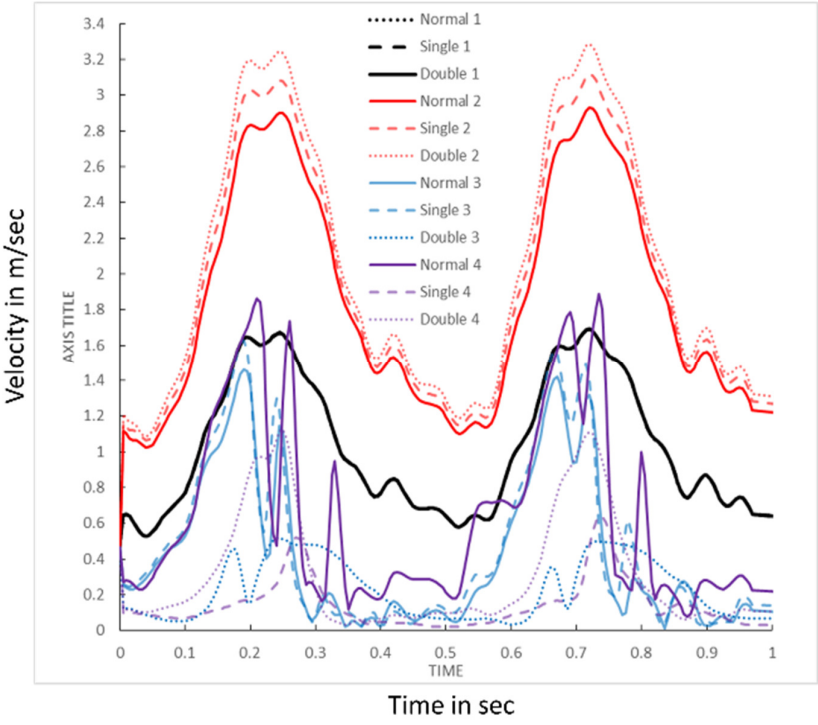

Fig. 9. Comparison of flow in pulse cycle during exercise condition in different models

Pressure distribution during peak systole is shown in the Figure 10 and 11 at rest and exercise conditions respectively in normal, single stenosed and double stenosed models. Maximum pressure in normal model is found to be at the proximal side, while low pressure at distal side of renal bifurcation tip in both the renal branches during entire pulse cycle. Upstream abdominal aorta also revealed higher pressure distribution in comparison with downstream side. Exercise condition had higher pressure build up in upstream side of abdominal aorta and also at the proximal side of renal bifurcation tip unlike rest condition. Pressure slightly drops at stenosed throat, while in the downstream side of stenosis it recovers gradually. Pressure in downstream side of stenosis recovers faster in exercise condition when compared with the rest condition.

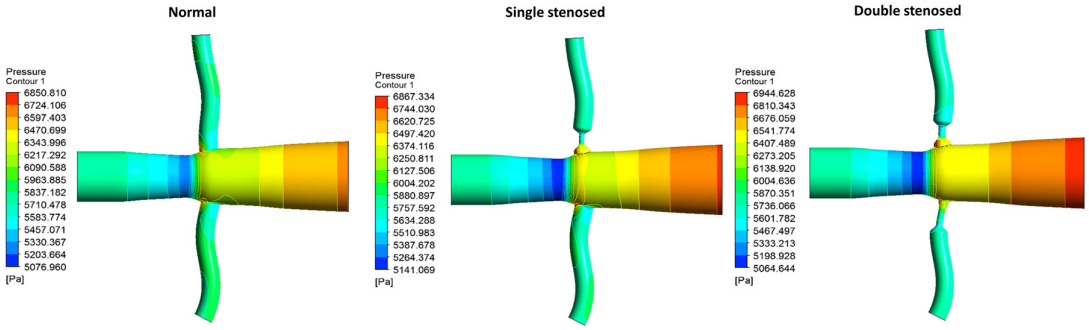

Fig. 10. Comparison of pressure contour during peak systole in rest condition in different models

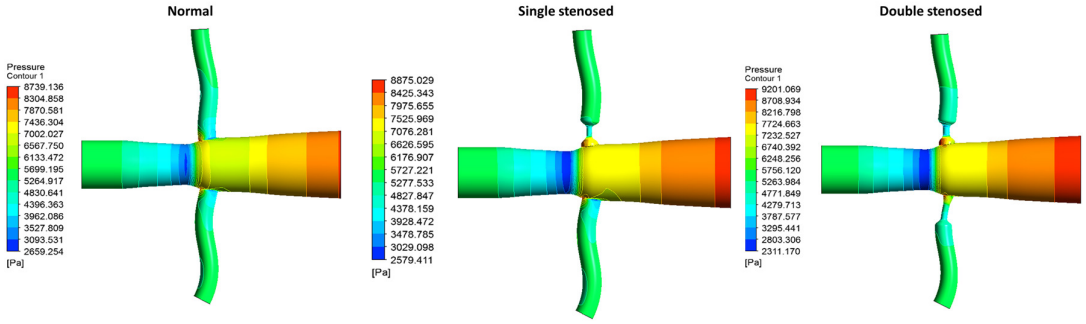

Fig. 11. Comparison of pressure contour during peak systole in exercise condition in different models

WSS behaviour during rest and exercise conditions is compared in the Figure 12 and 13 respectively in normal, single and double stenosed model. WSS in abdominal aorta wall of normal model tends to increase along its length in upstream side and especially at the branching of renal artery [12]. At the renal branch walls, the WSS distribution is found to be low along the proximal wall and the high WSS at the distal renal wall. The appearance of this low WSS in the proximal wall coincides with the presence of the recirculation. Along the distal wall, the WSS will be maximum in the entry of the bifurcation and tends to decrease along the distance. It is also observed that the distal wall in neighbourhood of bifurcation experience high WSS, whereas the proximal walls nearby the flow separation region suffer from relatively low WSS as observed clearly [23]. However, due to presence of stenosis, either as observed in single and double stenosed case, typical normal model maximum WSS behaviour at the distal walls side of renal branches is altered and appears to be maximum at the throat of the stenosis. Low WSS spread across the entire distal wall side on downstream of stenosis is also observed in contrast to the higher and low WSS spread along the distal and proximal wall side respectively in downstream side of normal renal branch. WSS behaviour

observed at renal bifurcation in distal side and at the throat of stenosis is relatively more intense during exercise when compared with rest conditions.

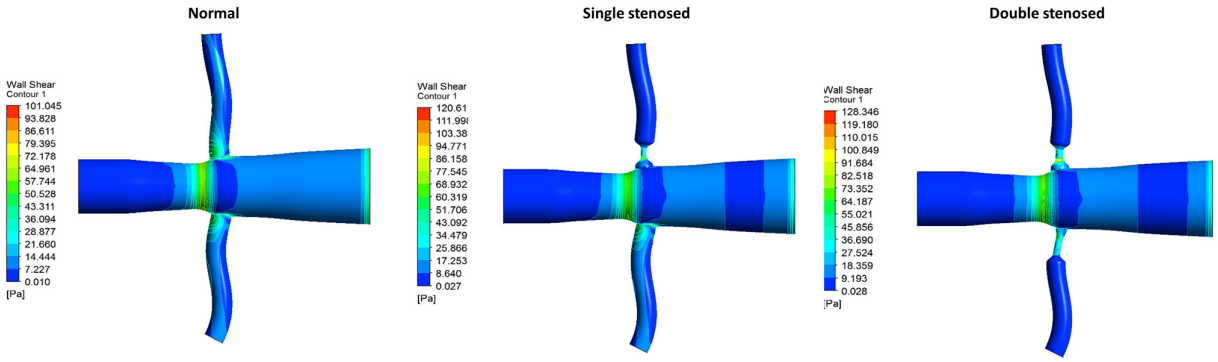

Fig. 12. Comparison of WSS during peak systole in rest condition in different models

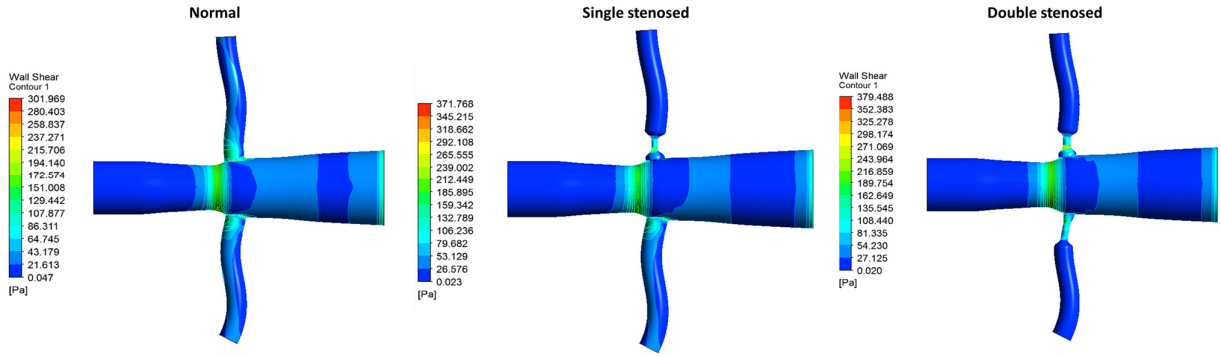

Fig. 13. Comparison of WSS during peak systole in exercise condition in different models

4. Conclusions

Numerically simulation of abdominal aorta branching into renal artery under rest and exercise conditions is carried out for normal, single and double stenosed models in this present study. The inflow is higher during peak systole in cardiac cycle and flow decelerates during diastole. Flow recirculation is observed in proximal side during rest which reduces significantly during exercise condition. However, high flow velocity is relatively low in rest while more intense during exercise condition. Flow behaviour in stenosis site is characterized by increased velocity at throat site. In rest conditions, flow jet at stenosed throat extends relatively to longer distance in double stenosed branches when compared to that in single stenosed branch. In exercise condition, there is significant change in the flow jet extending to longer length in contrast to that in rest condition. Flow velocity profile in downstream side of abdominal aorta has altered in double and single stenosed case when compared with the normal case which is found to be more intense in exercise condition in contrast to rest condition. WSS in renal branches is found to be low along the proximal wall and the high WSS at the distal renal wall. However, due to presence of stenosis, either in single and double stenosed case, maximum WSS will be at the throat of the stenosis unlike in typical normal model, maximum WSS is found to be at the distal walls side of renal branches. WSS behaviour observed at renal bifurcation in distal side and at the throat of stenosis is relatively more intense during exercise when compared with rest conditions. The present study demonstrates the fundamental aspects of haemodynamics in idealized normal and renal branch stenosed abdominal aorta. This study can be further extended to evaluate effect of rest and exercise conditions in the patient specific cases.

Acknowledgement
Authors acknowledge the support by Fundamental Research Grant Scheme (FRGS/1/2015/TK03/ MIU/02/1).

References
[1] Ku, David N. "Blood flow in arteries." *Annual review of fluid mechanics* 29, no. 1 (1997): 399-434.
[2] Marshall, Ian, Shunzhi Zhao, Panorea Papathanasopoulou, Peter Hoskins, and X. Yun Xu. "MRI and CFD studies of pulsatile flow in healthy and stenosed carotid bifurcation models." *Journal of biomechanics* 37, no. 5 (2004): 679-687.
[3] Antiga, Luca. "Patient-specific modeling of geometry and blood flow in large arteries." *Politecnico di Milano* (2002).
[4] Bai-Nan, Xu, Wang Fu-Yu, Liu Lei, Zhang Xiao-Jun, and Ju Hai-Yue. "Hemodynamics model of fluid–solid interaction in internal carotid artery aneurysms." *Neurosurgical review* 34, no. 1 (2011): 39-47.
[5] Xiong, Yan, Xuhong Wang, Wentao Jiang, Xiaobao Tian, Qingyuan Wang, Yubo Fan, and Yu Chen. "Hemodynamics study of a multilayer stent for the treatment of aneurysms." *Biomedical engineering online* 15, no. 2 (2016): 134.
[6] Mortazavinia, Z., S. Arabi, and A. R. Mehdizadeh. "Numerical Investigation of Angulation Effects in Stenosed Renal Arteries." *Journal of biomedical physics & engineering* 4, no. 1 (2014): 1.
[7] Albert, Scott, Robert S. Balaban, Edward B. Neufeld, and Jenn Stroud Rossmann. "Influence of the renal artery ostium flow diverter on hemodynamics and atherogenesis." *Journal of biomechanics* 47, no. 7 (2014): 1594-1602.
[8] Zhang, Weisheng, Yi Qian, Jiang Lin, Peng Lv, Kaavya Karunanithi, and Mengsu Zeng. "Hemodynamic analysis of renal artery stenosis using computational fluid dynamics technology based on unenhanced steady-state free precession magnetic resonance angiography: preliminary results." *The international journal of cardiovascular imaging*30, no. 2 (2014): 367-375.
[9] Mortazavinia, Z., A. Zare, and A. Mehdizadeh. "Effects of renal artery stenosis on realistic model of abdominal aorta and renal arteries incorporating fluid-structure interaction and pulsatile non-Newtonian blood flow." *Applied Mathematics and Mechanics* 33, no. 2 (2012): 165-176.
[10] Taylor, Charles A., Thomas JR Hughes, and Christopher K. Zarins. "Effect of exercise on hemodynamic conditions in the abdominal aorta." *Journal of vascular surgery* 29, no. 6 (1999): 1077-1089.
[11] Lee, Denz, and J. Y. Chen. "Numerical simulation of steady flow fields in a model of abdominal aorta with its peripheral branches." *Journal of Biomechanics* 35, no. 8 (2002): 1115-1122.
[12] Lee, D., and J. Y. Chen. "Pulsatile flow fields in a model of abdominal aorta with its peripheral branches." *Biomedical Engineering: Applications, Basis and Communications* 15, no. 05 (2003): 170-178.
[13] Suh, Ga-Young, Andrea S. Les, Adam S. Tenforde, Shawn C. Shadden, Ryan L. Spilker, Janice J. Yeung, Christopher P. Cheng, Robert J. Herfkens, Ronald L. Dalman, and Charles A. Taylor. "Quantification of particle residence time in abdominal aortic aneurysms using magnetic resonance imaging and computational fluid dynamics." *Annals of biomedical engineering* 39, no. 2 (2011): 864-883.
[14] Taylor, Charles A., Thomas JR Hughes, and Christopher K. Zarins. "Finite element modeling of three-dimensional pulsatile flow in the abdominal aorta: relevance to atherosclerosis." *Annals of biomedical engineering* 26, no. 6 (1998): 975-987.
[15] Suh, Ga-Young, Andrea S. Les, Adam S. Tenforde, Shawn C. Shadden, Ryan L. Spilker, Janice J. Yeung, Christopher P. Cheng, Robert J. Herfkens, Ronald L. Dalman, and Charles A. Taylor. "Hemodynamic changes quantified in abdominal aortic aneurysms with increasing exercise intensity using MR exercise imaging and image-based computational fluid dynamics." *Annals of biomedical engineering* 39, no. 8 (2011): 2186-2202.
[16] Les, Andrea S., Shawn C. Shadden, C. Alberto Figueroa, Jinha M. Park, Maureen M. Tedesco, Robert J. Herfkens, Ronald L. Dalman, and Charles A. Taylor. "Quantification of hemodynamics in abdominal aortic aneurysms during rest and exercise using magnetic resonance imaging and computational fluid dynamics." *Annals of biomedical engineering* 38, no. 4 (2010): 1288-1313.
[17] Kagadis, George C., Eugene D. Skouras, George C. Bourantas, Christakis A. Paraskeva, Konstantinos Katsanos, Dimitris Karnabatidis, and George C. Nikiforidis. "Computational representation and hemodynamic characterization of in vivo acquired severe stenotic renal artery geometries using turbulence modeling." *Medical engineering & physics* 30, no. 5 (2008): 647-660.
[18] Moore Jr, James E., Chengpei Xu, Seymour Glagov, Christopher K. Zarins, and David N. Ku. "Fluid wall shear stress measurements in a model of the human abdominal aorta: oscillatory behavior and relationship to atherosclerosis." *Atherosclerosis* 110, no. 2 (1994): 225-240.
[19] Y. Fung (1984), Chapter-1- Principles of Circulation, Chapter-3 – Blood Flow in Arteries, Biodynamics-Circulation, Page 1-21, 77-165.
[20] J. Ferziger, M. Peric (2002). Chapter 1- Basic Concepts of Fluid Flow, Computational Methods for Fluid Dynamics,

Page 1-12.
[21] ANSYS Release 17.0 Documentation (2016), ANSYS Company, Pittsburgh, PA.
[22] LIANG, Fuyou, Ryuhei YAMAGUCHI, and Hao LIU. "Fluid dynamics in normal and stenosed human renal arteries: an experimental and computational study." *Journal of Biomechanical Science and Engineering* 1, no. 1 (2006): 171-182.
[23] Khader, Abdul SM, Satish B. Shenoy, Raghuvir B. Pai, Ganesh S. Kamath, Nabeel Md Sharif, and V. R. K. Rao. "Effect of increased severity in patient specific stenosis of common carotid artery using CFD—a case study." *World Journal of Modelling and Simulation* 7, no. 2 (2011): 113-122.
[24] Azam, M. A., and S. A. A. Salam. "Three Dimensional Analysis of the Blood Flow Regime within Abdominal Aortic Aneurysm." *International Journal of Engineering and Technology* 3, no. 6 (2011): 621.